Differentiation of β-Sheet-Forming Structures: Ab Initio-Based Simulations of IR Absorption and Vibrational CD for Model Peptide and Protein β-Sheets

Jan Kubelka and Timothy A. Keiderling*

Contribution from the Department of Chemistry (M/C 111), University of Illinois at Chicago, 845 West Taylor Street, Room 4500, Chicago, Illinois 60607-7061

Received July 9, 2001

Abstract: Ab initio quantum mechanical computations of force fields (FF) and atomic polar and axial tensors (APT and AAT) were carried out for triamide strands Ac-A-A-NH-CH_3 clustered into single-, double-, and triple-strand β-sheet-like conformations. Models with ϕ, ψ, and ω angles constrained to values appropriate for planar antiparallel and parallel as well as coiled antiparallel (two-stranded) and twisted antiparallel and parallel sheets were computed. The FF, APT, and AAT values were transferred to corresponding larger oligopeptide β-sheet structures of up to five strands of eight residues each, and their respective IR and vibrational circular dichroism (VCD) spectra were simulated. The antiparallel planar models in a multiple-stranded assembly give a unique IR amide I spectrum with a high-intensity, low-frequency component, but they have very weak negative amide I VCD, both reflecting experimental patterns seen in aggregated structures. Parallel and twisted β-sheet structures do not develop a highly split amide I, their IR spectra all being similar. A twist in the antiparallel β-sheet structure leads to a significant increase in VCD intensity, while the parallel structure was not as dramatically affected by the twist. The overall predicted VCD intensity is quite weak but predominantly negative (amide I) for all conformations. This intrinsically weak VCD can explain the high variation seen experimentally in β-forming peptides and proteins. An even larger variation was predicted in the amide II VCD, which had added complications due to non-hydrogen-bonded residues on the edges of the model sheets.

Introduction

Globular proteins, despite the vast diversity of their structures, have two main secondary structural types, α-helix and β-sheet. Unlike the α-helix, the β-sheet cannot be truly classified as a secondary structure, since it does not occur as a single β-strand, but rather as β-sheets which incorporate two or more associated strands. The β-sheet structure is stabilized by both intra- and interstrand (tertiary) interactions involving hydrogen-bonding and side-chain (hydrophobic) interactions, as well as by intersheet association of the hydrophobic sheet surfaces.[1] While the α-helix forms a relatively uniform and well-defined conformation (as concerns the ϕ, ψ torsional angles), the β-sheet encompasses a much broader conformational class, the diversity of which is further multiplied by a wide range of topologies resulting from different assemblies of multistranded arrays.[1,2] Due to these complications, understanding of the β-sheet conformation lags behind that of the α-helix. An example of this difference is the lack, until recently, of designed, solution-stable β-sheet peptides, as compared to the number of water-soluble α-helical peptide models.[3−6]

Infrared absorption (IR) spectroscopy is a classical technique long used for peptide and protein conformational analysis.[7−11] Even though it lacks the detailed residue-specific structural resolution of X-ray or NMR, the wide applicability, high sensitivity, and fast time response of IR spectroscopy have made it a valuable tool for estimation of average secondary structural content[12,13] and, importantly, for following structural changes in protein denaturation studies.[14−16] The interpretation of peptide and protein IR spectra is most commonly based on correlations of characteristic amide I (amide C═O stretch, 1600−1700 cm^{-1}) band frequencies with structure.[12,13,17] However, such assignments based on amide I IR frequencies can be misleading:[17,18]

* To whom correspondence should be addressed. Phone: (312) 996-3156. Fax: (312) 996-0431. E-mail: tak@uic.edu.

(1) Nesloney, C. L.; Kelly, J. W. *Bioorg. Med. Chem.* **1996**, *4*, 739.
(2) Salemme, F. R. *Prog. Biophys. Mol. Biol.* **1983**, *42*, 95.
(3) Marqusee, S.; Robbins, V. H.; Baldwin, R. L. *Proc. Natl. Acad. Sci. U.S.A.* **1989**, *86*, 5286.
(4) Scholtz, J. M.; Baldwin, R. L. *Annu. Rev. Biophys. Biomol. Struct.* **1992**, *21*, 95.
(5) Yoder, G.; Pancoska, P.; Keiderling, T. A. *Biochemistry* **1997**, *36*, 15123.
(6) Silva, R. A. G. D.; Kubelka, J.; Decatur, S. M.; Bour, P.; Keiderling, T. A. *Proc. Natl. Acad. Sci. U.S.A.* **2000**, *97*, 8318.
(7) Parker, F. S. *Applications of Infrared Spectroscopy in Biochemistry, Biology and Medicine*; Plenum Press: New York, 1971.
(8) Susi, H.; Byler, D. M. *Methods Enzymol.* **1986**, *130*, 290.
(9) Braiman, M. S.; Rothschild, K. J. *Annu. Rev. Biophys. Biophys. Chem.* **1988**, *17*, 541.
(10) Mantsch, H. H.; Chapman, D. *Infrared Spectroscopy of Biomolecules*; Wiley-Liss: Chichester, UK, 1996.
(11) Singh, B. R. In *Infrared Analysis of Peptides and Proteins: Principles and Applications*; Singh, B. R., Ed.; ACS Symposium Series; American Chemical Society: Washington, DC, 2000.
(12) Byler, D. M.; Susi, H. *Biopolymers* **1986**, *25*, 469.
(13) Surewicz, W.; Mantsch, H. H.; Chapman, D. *Biochemistry* **1993**, *32*, 389.
(14) Cowen, B. R.; Hochstrasser, R. M. *Infrared Spectroscopy of Biomolecules*; Wiley-Liss: Chichester, UK, 1996; p 107.
(15) Georg, H.; Wharton, C. W.; Siebert, F. *Laser Chem.* **1999**, *19*, 233.
(16) Troullier, A.; Reinstadler, D.; Dupont, Y.; Naumann, D.; Forge, V. *Nat. Struct. Biol.* **2000**, *7*, 78.
(17) Haris, P. I. In *Infrared Analysis of Peptides and Proteins: Principles and Applications*; Ram Singh, B., Ed.; ACS Symposium Series; American Chemical Society: Washington, DC, 2000; p 54.
(18) Jackson, M.; Mantsch, H. H. *Crit. Rev. Biochem. Mol. Biol.* **1995**, *30*, 95.

10.1021/ja0116627 CCC: $20.00
Published on Web 11/01/2001

for example, short α-helical oligopeptides whose amide I maximum is at ~1633 cm^{-1} might have been interpreted as β-sheets, if other data (such as circular dichroism) were not used as well.[5,6,19,20] Vibrational circular dichroism (VCD), on the other hand, adds characteristic signed band shape patterns to the frequency resolution of IR and therefore can provide a new dimension to biopolymer conformational interpretation.[21]

Historically, the amide I IR has been regarded as specifically sensitive to the β-sheet structure in polypeptides, with a characteristic intense low-frequency (~1620−1630 cm^{-1}) maximum and, in some cases, a weaker high-frequency (~1680−1690 cm^{-1}) peak.[7,17,18,22] This split pattern distinguishes it from other structures, whose amide I's are overlapped components forming single bands which are typically at higher frequencies than the intense β-sheet feature. However, it has been pointed out[17,18] that this "characteristic" amide I β-sheet IR band shape may actually be only typical for large, extended β-sheet aggregates, since it is observed only in model peptides and denatured proteins, but usually not in native proteins.

Early efforts at computing β-sheet IR spectra have predominantly focused on ideal, infinite periodic structures,[23,24] where the spectral pattern is fully determined by the single repeating unit. Later, full calculations on the finite ideal β-sheet structures[25] predicted a strong dependence of the amide I band shape on the number of associated strands as well as the strand length, the "characteristic" split pattern being approached in the limit of the infinite sheets. However, finite β-sheets no longer assume idealized periodic structures but develop a twist, where the smaller β-sheets typically have larger deviations. Thus, relatively small β-sheets that occur in native globular proteins are invariably twisted, assuming a wide variety of strand conformations as well as interstrand configurations.[1,2] If the band shapes are dependent on the detailed conformation of the β-strands, their lengths, and the number of associated strands in the β-sheet, a "typical" β-sheet spectral signature may not exist. No systematic study of predicted spectral band shapes is available for realistic, twisted structures such as those found in proteins; that is our goal here.

Specific conformational effects can be expected to be especially significant for the amide mode VCD, which is sensitive to helical conformations and shows very weak amide I signals for polypeptide β-sheets with the characteristic IR pattern.[26−28] In fact, in the limit of a hypothetical fully extended polypeptide chain (i.e., all-trans, $\phi = \psi = \omega = 180°$), the VCD signal for the amide modes would vanish, since the chirality of the amide backbone (neglecting the side chains) would be lost.[29] It is clear that variations in β-sheet structure can, in principle, have a large impact on the β-sheet VCD, resulting in substantial changes in intensities and band shapes. In addition, all globular proteins containing β-sheet structure also contain a substantial fraction of residues forming turns and loops connecting the β-sheet segments. These, due to their more chiral backbone conformation (locally helical), might be expected to yield relatively large VCD signals and lead to false interpretations. Detailed study of the spectral characteristics of β-sheets of different sizes and conformations is not available and is therefore needed.

In this report we compare quantum mechanically based simulations of IR and VCD spectra of model antiparallel and parallel β-sheets in different conformations and sizes. The heart of these simulations is the ab initio density functional theory (DFT) calculation of vibrational absorption and VCD parameters (atomic polar and axial tensors, APT and AAT, as well as force fields, FF) for a small oligopeptide and the transfer of these parameters onto a much larger, structurally related molecule using the property tensor transfer algorithm developed by Bour et al.[30] We have previously demonstrated that such simulations of oligopeptide IR and VCD for helical peptide structures show satisfactory agreement with experiment[6,29,31] and provide valuable insight into the nature of the observed spectra.

Simulations of vibrational spectra for β-sheets are substantially more complicated than are those for the α-helices. First, β-sheets generally require larger quantum mechanical calculations than the α-helices, if all important inter- and intrastrand interactions within the β-sheet fragment are to be included. Second, it is difficult to find suitable structural models for the β-sheets. For the parameter transfer method to be most useful, a peptide of uniform structure is needed that corresponds to that of the ab initio calculated small fragment. The planar antiparallel β-sheet structure of the crystalline poly-L-alanine[22] is conformationally regular and can be simply extended in both strand length and number of strands. [We refer to the β-sheet as "planar" when the strands are 2_1-helices (two residues per turn) as opposed to "twisted", where the strands are locally helical. Note, however, that a strictly planar structure corresponds to a fully extended chains (ϕ, ψ, $\omega = 180°$), while the β-sheets are invariably pleated, i.e., the successive amide groups in the strand are tilted.] Similar parallel β-sheet polypeptide models are not available. Twisted β-sheets found in proteins are conformationally irregular, since the hydrogen-bonding constraints prevent twisted β-sheets with a larger number of strands from preserving a regular conformation.[2] These constraints also impose natural limits on the degree of the twist of the β-sheets with respect to both the number and length of strands. Consequently, longer β-sheets and β-sheets with more strands twist less than those with shorter or fewer strands. A strictly regular twisted β-sheet structure is possible only for the double-stranded antiparallel configuration.[2] Highly uniform, multiply stranded parallel β-sheets can be found, particularly in β-helix-type domains of proteins,[1] but these are composed of relatively short β-strands. Therefore, while it would be interesting to study size effects in twisted β-sheets, the range of sizes and number of strands possible in a uniform structure are limited.

Consequently, we restricted our simulation studies of different lengths and number of strands in the β-sheet to uniform, periodic structures (Figure 1). As we have shown, extended antiparallel structures (Figure 1a) can serve as the simplest models for aggregated polypeptide β-sheets.[32] Due to the lack of an experimental structural model for a planar parallel β-sheet structure, we performed analogous simulations for different sizes

(19) Martinez, G.; Millhauser, G. *J. Struct. Biol.* **1995**, *114*, 23.
(20) Decatur, S. M.; Antonic, J. *J. Am. Chem. Soc.* **1999**, *121*, 11914.
(21) Keiderling, T. A. In *Circular dichroism: principles and applications*, 2nd ed.; Nakanishi, K., Berova, N., Woody, R. A., Eds.; Wiley: New York, 2000; p 621.
(22) Fraser, R. D. B.; McRae, T. P. *Conformation in Fibrous Proteins*; Academic Press: New York, 1973.
(23) Miyazawa, T. *J. Chem. Phys.* **1960**, *32*, 1647.
(24) Krimm, S.; Abe, Y. *Proc. Natl. Acad. Sci. U.S.A.* **1972**, *69*, 2788.
(25) Chirgadze, Y. N.; Nevskaya, N. A. *Biopolymers* **1976**, *15*, 607.
(26) Yasui, S. C.; Keiderling, T. A. *J. Am. Chem. Soc.* **1986**, *108*, 5576.
(27) Paterlini, M. G.; Freedman, T. B.; Nafie, L. A. *Biopolymers* **1986**, *25*, 1751.
(28) Baumruk, V.; Huo, D. F.; Dukor, R. K.; Keiderling, T. A.; Lelievre, D.; Brack, A. *Biopolymers* **1994**, *34*, 1115.
(29) Kubelka, J.; Silva, R. A. G. D.; Bour, P.; Decatur, S. M.; Keiderling, T. A. In *The Physical Chemistry of Chirality*; Hicks, J. M., Ed.; ACS Symposium Series; Oxford University Press: New York, 2001 (in press).
(30) Bour, P.; Sopkova, J.; Bednarova, L.; Malon, P.; Keiderling, T. A. *J. Comput. Chem.* **1997**, *18*, 646.
(31) Bour, P.; Kubelka, J.; Keiderling, T. A. *Biopolymers* **2000**, *53*, 380.
(32) Kubelka, J.; Keiderling, T. A. *J. Am. Chem. Soc.* **2001**, *123*, 6142.

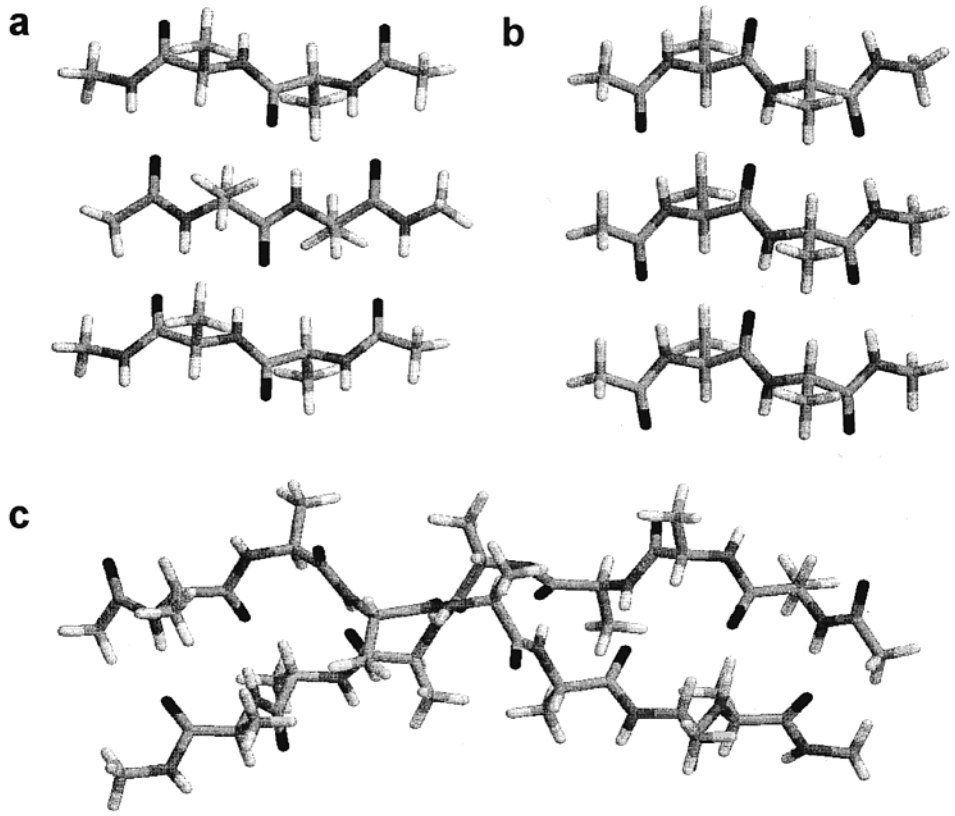

Figure 1. Models of the regular β-sheet structures used for spectral simulations. (a) Antiparallel β-sheet segment with three triamide strands (3 × 3) based on the crystal structure of poly-L-alanine; (b) parallel planar β-sheet with three triamide strands (3 × 3) based on standard ϕ, ψ, ω values; (c) antiparallel supercoiled β-sheet with two octaamide strands (2 × 8) based on an idealized segment of BPTI (Table 1). The 3 × 3 amide segments were used in ab initio calculations.

Table 1. Structural Parameters for Model β-Sheets Used for Spectral Simulations

type of β-sheet	torsional angles (deg) ϕ	ψ	ω	H-bond distance (O···H) (Å)	source
antiparallel planar	138.6	134.5	178.5	1.898	poly-L-Ala (X-ray)[22]
parallel planar	119	113	180	1.948	standard values[33]
antiparallel supercoiled[a]	114 (S) 92 (L)	150 (S) 114 (L)	180	1.835	idealized segment of bovine pancreatic trypsin inhibitor (BPTI)[2]
antiparallel twisted[b]	105−149	120−153	173−171	1.81−2.15	intestinal fatty acid binding protein (PDB code 1IFC)[34] residues: 102−109, 112−119, 122−129
parallel twisted[b]	111−135	102−145	179−176	1.89−2.29	pectate lyase C (PDB code 2PEC)[35] residues: 112−116, 140−144, 177−181, 204−208, 225−230

[a] S and L refer to small and large hydrogen bonds, respectively. [b] In structures from proteins, torsional angles vary, so ranges are presented.

of hypothetical planar parallel β-sheets constructed using standard ϕ, ψ values[33] (Figure 1b). To study effects of the β-sheet twist, we simulated spectra of an idealized, highly coiled two-stranded antiparallel β-sheet model (Figure 1c). Finally, to estimate the differences between the spectra of these regular models and real twisted protein β-sheet structures, IR and VCD spectra were simulated for an antiparallel and a parallel β-sheet structure, taken from the crystal structures of two selected proteins (Figure 2).

Methods

Model Peptides. All antiparallel β-sheet models, whose spectra were simulated by transfer of the ab initio force fields (FF), atomic polar (APT), and atomic axial (AAT) tensors, were composed of strands containing eight amide bonds (octaamides) with the sequence Ac-A_7-NH-CH_3 (A = Ala) and are referred to as "large". All corresponding smaller antiparallel β-sheets used in ab initio calculations were constructed from Ac-A_2-NH-CH_3 strands (triamides) and are referred to as "small". For easier reference, the adopted structural models are summarized in Table 1.

Planar antiparallel β-strand and β-sheet models (Figure 1a) were derived using uniform ϕ, ψ, ω torsional angles and H-bond distances from the crystal structure of β-sheet poly-L-alanine (Table 1),[22] and planar parallel β-sheet models (Figure 1b) were constructed using the standard ϕ, ψ, ω values (Table 1).[33]

Supercoiled two-stranded antiparallel β-sheet segments (Figure 1c) were constructed using pairs of torsional angles ϕ_S, ψ_S, ϕ_L, and ψ_L (Table 1), where the subscripts S and L denote the small and large interstrand hydrogen bond rings, respectively, which approximate a segment of the bovine pancreatic trypsin inhibitor protein (BPTI).[2]

For protein-related models of twisted two- and three-stranded β-sheet geometries, a segment was taken from the intestinal fatty acid binding protein (PDB code 1IFC) structure,[34] which contains a large antiparallel β-barrel domain (with a range of ϕ, ψ angles as in Table 1). Residues 112−119 and 122−129, corresponding to two adjacent strands in the

(33) Creighton, T. E. *Proteins: Structures and Molecular Properties*, 2nd ed.; W. H. Freeman and Co.: New York, 1993.

(34) Scapin, G.; Gordon, J. I.; Sacchettini, J. C. *J. Biol. Chem.* **1992**, *267*, 4253.

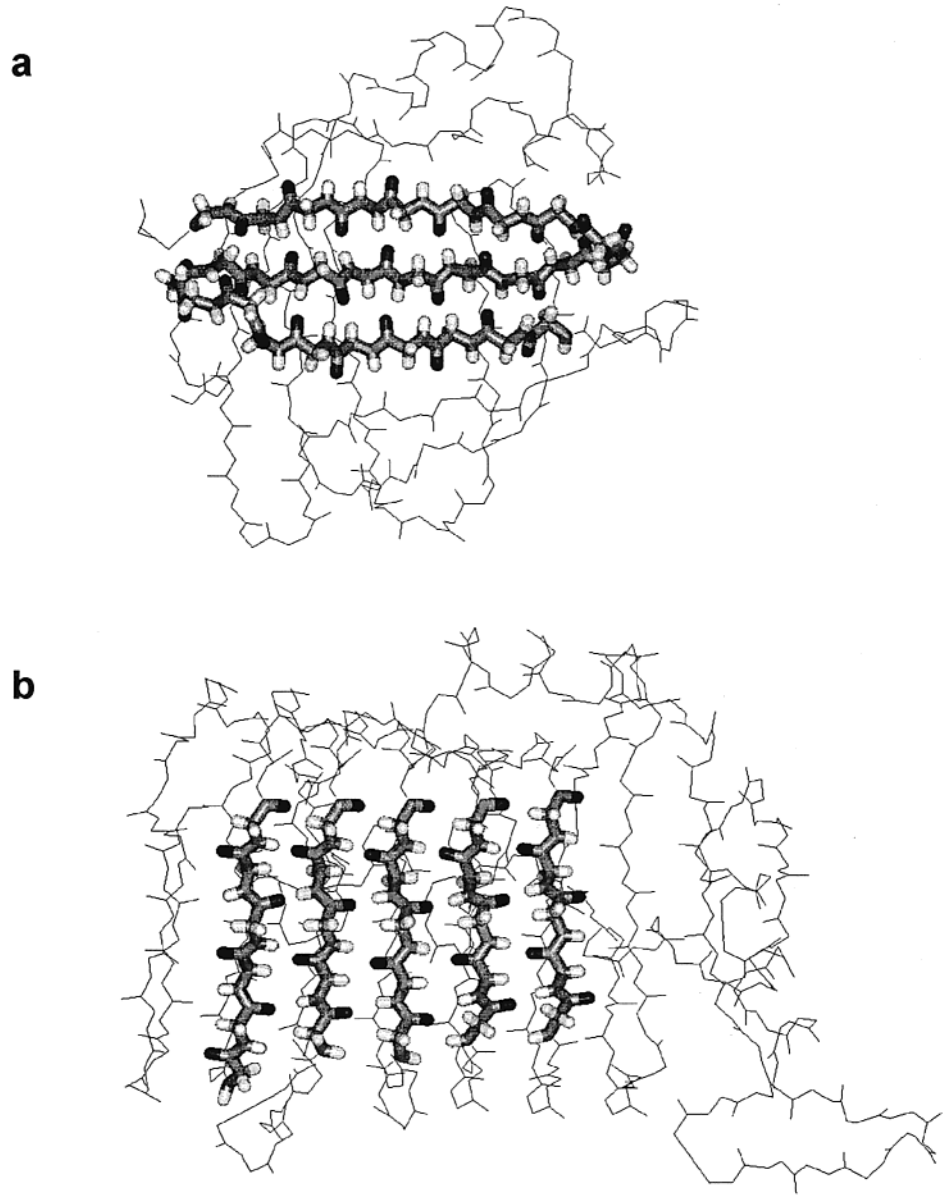

Figure 2. Protein segments used as model twisted β-sheet structures for spectral simulations (Table 1). (a) Antiparallel β-sheet segment (residues 102−109, 112−119, 122−129, in stick representation) of the intestinal fatty acid binding protein (PDB code 1IFC); (b) parallel β-sheet segment (residues 112−116, 140−144, 177−181, 204−208, 225−230, in stick representation) of the pectate lyase C (PDB code 2PEC).

protein β-sheet, with side-chains replaced by $-CH_3$ (Ala) and terminally capped (thus adjusted to the general sequence Ac-A_7-NH-CH_3), were used as the two-stranded large model. The corresponding small peptide was taken from the center three residues of this molecule. The three-stranded large oligopeptide additionally included residues 102−109 of 1IFC (Figure 2a), and its central part was again taken as the corresponding small peptide.

Twisted large parallel β-sheet models were constructed on the basis of a β-helix protein pectate lyase (PDB code 2PEC, Table 1).[35] Two-, three-, and five-stranded parallel β-sheets composed of pentaamide strands (Ac-A_4-NH-CH_3) were simulated using parameters from the corresponding small peptides. A five-stranded parallel β-sheet model corresponds to the protein segment of residues 112−116, 140−144, 177−181, 204−208, and 225−230 (Figure 2b). The three middle strands were taken as the model of the three-stranded large peptide and the 140−144 and 177−181 strands for the two-stranded model. The corresponding small peptide geometries were again obtained from the middle of the corresponding larger structures.

Ab Initio Calculations. Density functional theory (DFT), BPW91/6-31G** level computations for two- and three-stranded β-sheet structures composed of Ac-A_2-NH-CH_3 strands used Gaussian 98.[36] First, partial geometry optimization was performed, with only the backbone torsional angles (ϕ, ψ, ω) constrained to the initial values, until the full, default convergence criteria were met. Analytical harmonic force fields (FF), atomic polar tensors (APT), and atomic axial tensors (AAT), using magnetic field perturbation (MFP) theory[37] with gauge-independent atomic orbitals (GIAO)[38] as implemented in Gaussian 98,[39]

(35) Yoder, M. D.; Jurnak, F. *Plant. Physiol.* **1995**, *107*, 349.

(36) Frisch, M. J.; Trucks, G. W.; Schlegel, H. B.; Scuseria, G. E.; Robb, M. A.; Cheeseman, J. R.; Zakrzewski, V. G.; Montgomery, J. A., Jr.; Stratmann, R. E.; Burant, J. C.; Dapprich, S.; Millam, J. M.; Daniels, A. D.; Kudin, K. N.; Strain, M. C.; Farkas, O.; Tomasi, J.; Barone, V.; Cossi, M.; Cammi, R.; Mennucci, B.; Pomelli, C.; Adamo, C.; Clifford, S.; Ochterski, J.; Petersson, G. A.; Ayala, P. Y.; Cui, Q.; Morokuma, K.; Malick, D. K.; Rabuck, A. D.; Raghavachari, K.; Foresman, J. B.; Cioslowski, J.; Ortiz, J. V.; Stefanov, B. B.; Liu, G.; Liashenko, A.; Piskorz, P.; Komaromi, I.; Gomperts, R.; Martin, R. L.; Fox, D. J.; Keith, T.; Al-Laham, M. A.; Peng, C. Y.; Nanayakkara, A.; Gonzalez, C.; Challacombe, M.; Gill, P. M. W.; Johnson, B. G.; Chen, W.; Wong, M. W.; Andres, J. L.; Head-Gordon, M.; Replogle, E. S.; Pople, J. A. *Gaussian 98*, revision A.6; Gaussian, Inc.: Pittsburgh, PA, 1998.

(37) Stephens, P. J. *J. Phys. Chem.* **1985**, *89*, 748.

(38) Bak, K. L.; Jorgensen, P.; Helgaker, T.; Ruud, K.; Jensen, H. J. *J. Chem. Phys.* **1993**, *98*, 8873.

were then computed. The calculation of the largest, three-stranded peptide (96 atoms, 45 heavy atoms, 930 basis functions) took 10−15 days using 4 CPUs of the UIC computer center HP 9000/800 server. (It can be noted that these three-stranded β-sheets containing nine peptide units may be the largest molecules, to date, for which fully ab initio VCD spectra have been calculated.)

Transfer of the Property Tensors. Vibrational spectra of larger β-sheet models (up to five octaamide strands) were simulated by transfer of the ab initio-calculated FF, APT, and AAT matrices in Cartesian coordinates from the smaller (triamide strands) peptides, using programs written in-house following the method developed by Bour et al.[30] Ab initio-calculated FF, APT, and AAT values for the single-strand smaller peptide were transferred onto single-strand larger β-strands, and tensors from the two-stranded smaller peptide were transferred onto the two-stranded larger β-sheet. For both three- and five-stranded β-sheets, transfer from the three-stranded smaller peptide was used. In the five-stranded case, the tensor values from the inner strand of the small molecule were transferred onto all three inner strands, while values from the outer strands transferred to the outer strands of the large molecule.

Simulation of the Spectra. Simulation of the IR absorption and VCD spectra from molecular coordinates and FF, APT, and AAT values was performed using a set of programs written in-house. To remove the computed vibrational overlap and interference in the VCD from the rigid $-CH_3$ groups, deuterium was substituted for all methyl hydrogens. Experimentally, such side chains pose no interference, so that computational "removal" is the best way to mimic experiment. Effects of varied isotope substituents can also be studied, as we have previously demonstrated.[6,29,32] Resulting spectral band shapes, with intensities in ϵ ($M^{-1}cm^{-1}$) units, were simulated from the ν, D, and R values by summing Lorentzian line shapes with a uniform width (fwhm) of 15 cm^{-1} assigned to all transitions.

Results

Planar Antiparallel β-Sheets. The fully ab initio-simulated IR absorption and VCD spectra over the 1850−1200 cm^{-1} range for the triamide and heptaamide single β-strands, as well as two- and three-stranded β-sheets composed of triamide strands, are shown in Figure 3. The single β-strand IR spectrum shows a split amide I band with its main maximum due to the out-of-phase amide I vibration (mostly C═O stretch) of neighboring amides. A secondary maximum only ∼25 cm^{-1} higher is due to an in-phase mode. The single-strand amide II band (in-phase C−N stretch and N−H bend) is predicted around 210 cm^{-1} lower and with significantly more intensity than that of the amide I. The band at ∼1342 cm^{-1} is predominantly due to C^{α}−H bending mixed with amide III (out-of-phase C−N stretch and N−H bend), and the weak band at ∼1222 cm^{-1} is mostly amide III with some contribution of C^{α}−H motion. The amide I VCD is weak, negative, and shifted toward the higher frequency part of the absorption band, while the amide II VCD is a stronger negative couplet (negative then positive going to higher wavenumber). Positive and negative VCD corresponds to the C^{α}−H (amide III) and amide III absorption maxima, respectively. The fully ab initio-simulated single heptaamide β-strand spectra are similar to those of the triamide (Figure 3b).

The simulated spectra for a β-sheet composed of two triamide strands have some significant frequency and intensity differences from the single β-strand results. The amide I maximum shifts down about 20 cm^{-1}, while the amide II band shifts up about 25 cm^{-1} in frequency. The intensity of the low-frequency amide I maximum increases, dominating the spectrum (the amide II and III decrease), and its splitting increases to ∼30 cm^{-1}. The three-stranded β-sheet IR spectra show broader and more complex bands, with an additional peak near the center of the amide I band contour and a shift of its main maximum lower, further splitting the amide I band and lowering the amide I−II separation.

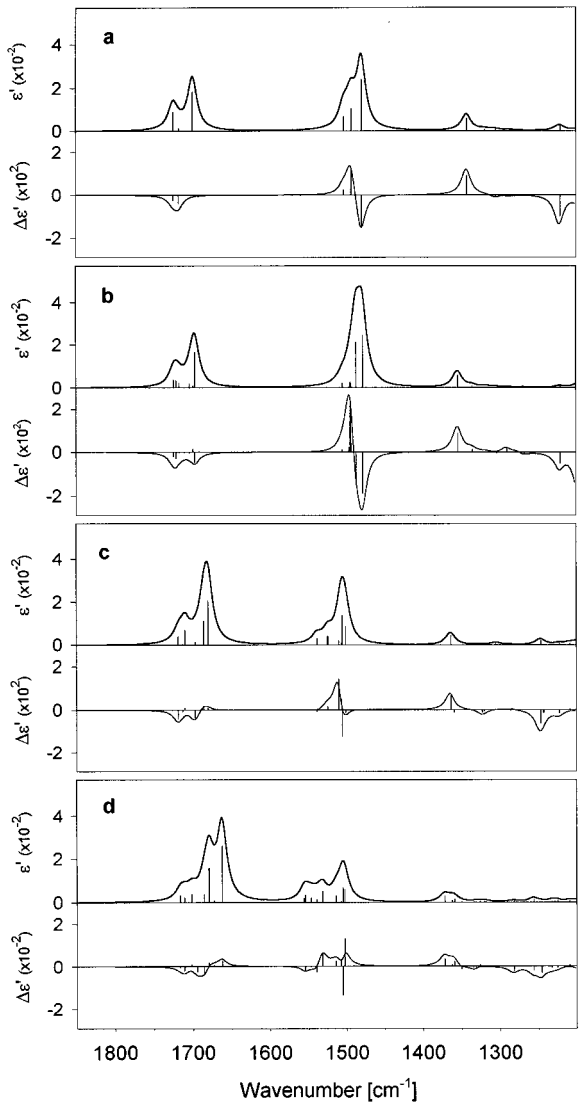

Figure 3. Ab initio simulated IR (in units of ϵ': molar extinction coefficient per amide group) and VCD (in units of $\Delta\epsilon$': differential molar extinction coefficient per amide group) spectra for antiparallel β-sheet structures based on the crystal structure of the β-form of poly-L-alanine (Table 1). (a) Triamide β-strand (Ac-A_2-NH-CH_3); (b) heptaamide β-strand (Ac-A_6-NH-CH_3); (c) two-stranded β-sheet with triamide strands (2 × Ac-A_2-NH-CH_3); (d) three-stranded β-sheet with triamide strands (3 × Ac-A_2-NH-CH_3).

The spectral simulations for the antiparallel β-sheet models composed of octaamide strands, carried out using the transfer of property tensors from the short fragments, are shown in Figure 4. The single octaamide β-strand spectrum is virtually identical to that of the ab initio-simulated heptaamide strand, which confirms the validity of the transfer method[30] for these molecules. The IR and VCD spectra of the large two-stranded (2 × 8) construct are similar to those of the small (2 × 3) model with slightly smaller amide I−II separation and slightly different intensities. Similar effects can be observed in the three-stranded β-sheet models, which confirms the dominance of local interactions in determining these vibrational spectral characteristics. In the long (3 × 8) model the split amide II IR corresponds to the amides with hydrogen-bonded N−H groups (high-frequency component) and amides with non-hydrogen-bonded N−H's (low

(39) Stephens, P. J.; Devlin, F. J.; Chabalowski, C. F.; Frisch, M. J. *J. Phys. Chem.* **1994**, *98*, 11623.

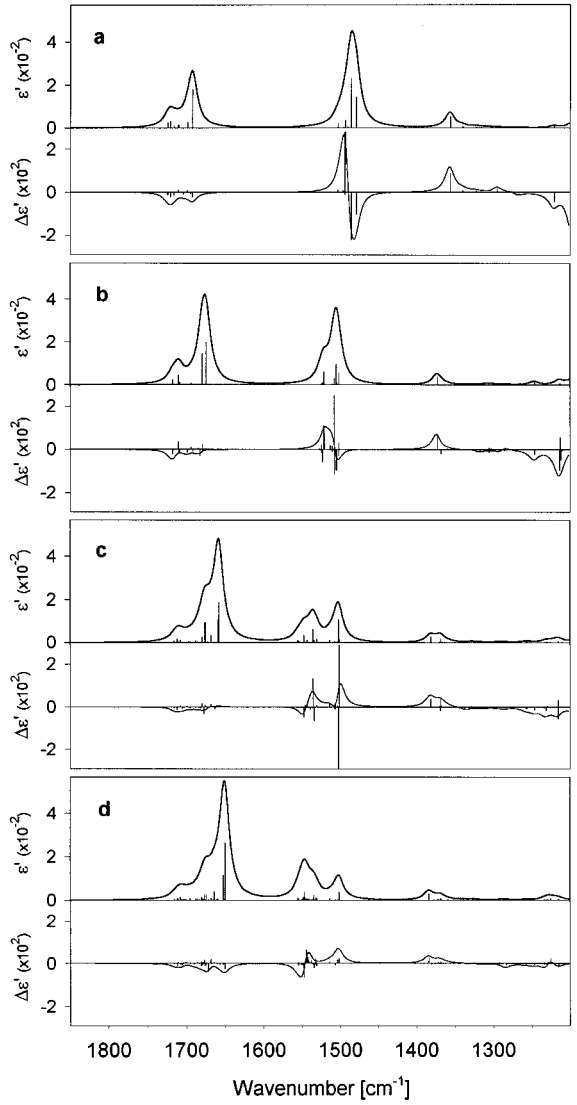

Figure 4. Simulated IR and VCD spectra of antiparallel β-sheet structures based on the crystal structure of β-form of poly-L-alanine (Table 1), by transfer of parameters from ab initio calculations. (a) Octaamide β-strand (Ac-A_7-NH-CH_3); (b) two-stranded β-sheet; (c) three-stranded β-sheet; and (d) five-stranded β-sheet, all β-sheets with octaamide strands (Ac-A_7-NH-CH_3). Spectral intensity units (ϵ', $\Delta\epsilon$') as in Figure 3.

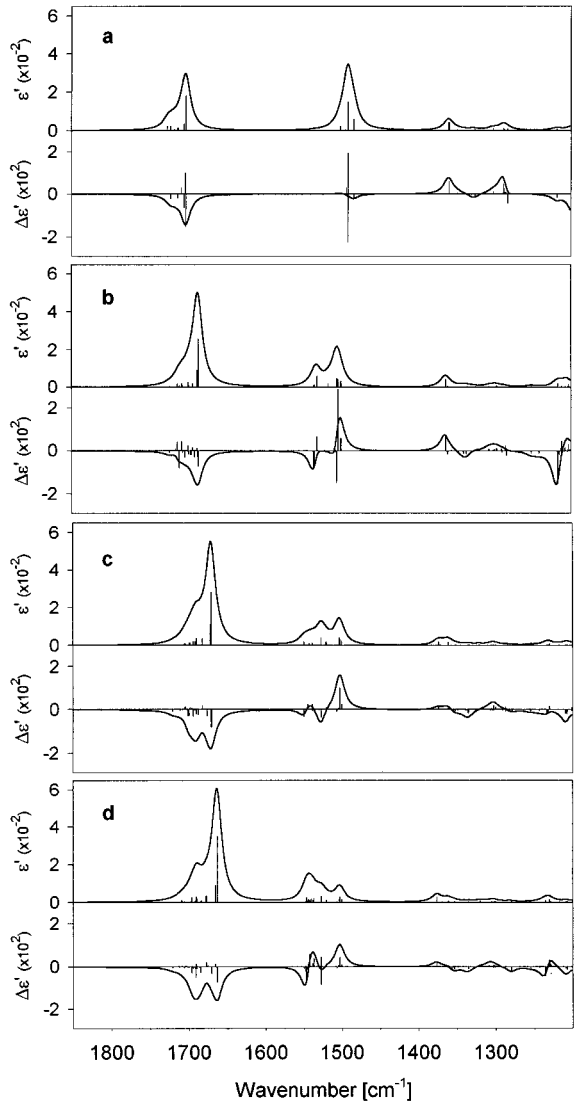

Figure 5. Simulated IR and VCD spectra for planar parallel β-sheets based on standard ϕ, ψ, ω values (Table 1), by transfer of parameters from ab initio calculations. (a) Octaamide β-strand; (b) two-stranded β-sheet; (c) three-stranded β-sheet; and (d) five-stranded β-sheet, all β-sheets with octaamide strands (Ac-A_7-NH-CH_3). Spectral intensity units (ϵ', $\Delta\epsilon$') as in Figure 3.

frequency). The amide I VCD remains a weak, broad negative. In the five-stranded (5×8) β-sheet model, the trends in the IR spectrum continue with an increase of the amide I splitting ($\sim$70 cm^{-1}) and intensity and a lowering of its maximum frequency, while amide II intensity shifts to higher frequency. In contrast to the IR, the VCD further decreases in intensity.

Planar Parallel β-Sheets. The simulated IR and VCD spectra for planar parallel β-sheet models composed of octaamide strands in a single strand and two-, three-, and five-stranded configurations are shown in Figure 5. The ab initio triamide results are not shown, since amide I and II frequencies and IR intensities follow the same trends with increasing length and number of the strands as those already described for the antiparallel case, and no significant differences from the long models occur in the VCD.

The IR spectra for the parallel β-sheet models are qualitatively similar to those for the antiparallel β-sheets, but with a few important differences. First, the parallel amide I components have a smaller splitting, and the main absorption maximum occurs at higher frequency. Second, the high-frequency amide I components shift down with the lower frequency modes on an increase in the number of strands so that the component splitting in the amide I does not increase as significantly as in the antiparallel models. Even more dramatic differences are seen in the simulated amide I VCD spectra, which are significantly more intense for parallel sheets and are in all cases negative. Different amide II VCD band shapes are predicted for the parallel β-sheets (except for a single strand), but by five-strands the amide II has nearly identical VCD to the antiparallel (5×8) model. The parallel amide III VCD region is more complex, and its intensity again decreases with the number of strands.

Regular Twisted ("Supercoiled") Antiparallel β-Sheet. The simulated IR and VCD spectra for the single octaamide strand and a two-stranded sheet in the supercoiled conformation are shown in Figure 6. The most important differences in the IR as compared to the corresponding planar models (Figure 4a,b) are the significantly less component splitting and different intensity distribution among the normal modes in the amide I of the supercoiled structures. As a consequence, the amide I IR

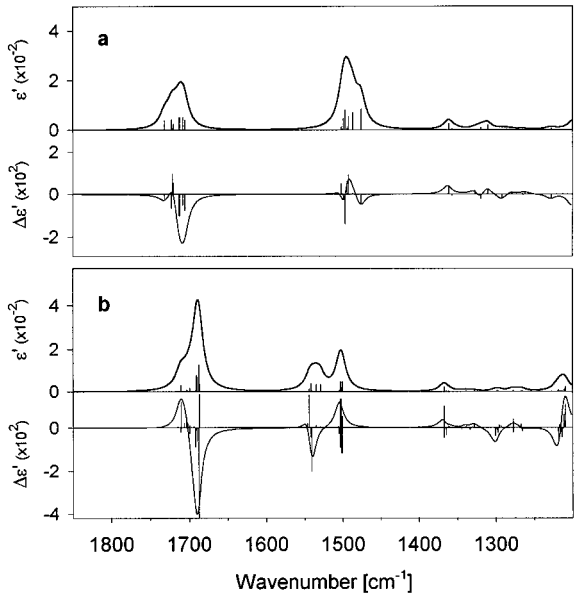

Figure 6. Simulated IR and VCD spectra for a supercoiled β-sheet structure based on a segment of BPTI. (a) Heptaamide β-strand (Ac-A_6-NH-CH_3); (b) two-stranded β-sheet with octaamide strands (2 × Ac-A_7-NH-CH_3). Spectra in (a) were simulated ab initio, spectra in (b) by transfer of parameters from two triamide strands in the supercoil conformation. Spectral intensity units (ϵ', $\Delta\epsilon$') as in Figure 3.

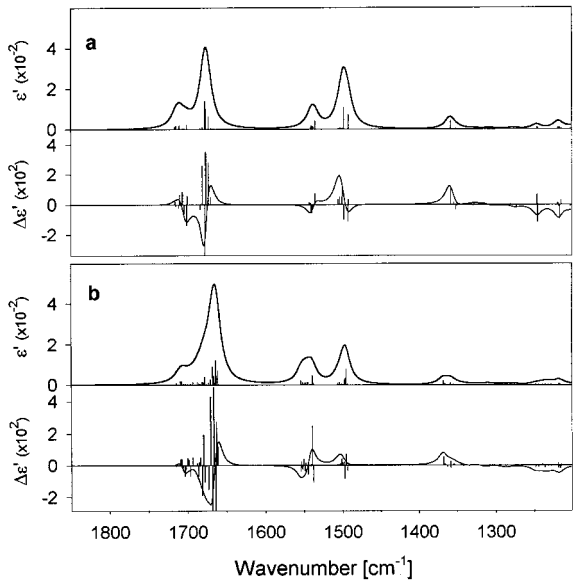

Figure 7. Simulated IR and VCD spectra for twisted antiparallel β-sheet structures based on a segment of intestinal fatty acid binding protein (1IFC, Table 1), by transfer of parameters from ab initio calculations. (a) Two-stranded and (b) three-stranded β-sheet, both with octaamide strands (Ac-A_7-NH-CH_3). Spectral intensity units (ϵ', $\Delta\epsilon$') as in Figure 3.

maximum occurs at higher frequency than that of the corresponding planar β-sheets. In the supercoiled models, the most IR intense amide I mode is not the lowest frequency one, as in the planar β-sheets, and its relative intensity is not as significantly greater compared to the remaining modes. A dramatic increase in amide I VCD intensity, more than an order of magnitude, is predicted for the supercoiled structures with respect to the planar model. The two-stranded coiled β-sheet amide I VCD has a negatively biased, negative couplet shape, similar to that found for the left-handed, 3_1-(ProII-like) helical conformation,[6,21,40] as compared to the more uniformly negative VCD for planar models.

Twisted Antiparallel β-Sheets. The simulated IR and VCD spectra for two- and three-stranded β-sheet segments with octaamide strands whose geometries are taken from the β-sheet of the intestinal fatty acid binding protein, are shown in Figure 7. Twisted β-sheet IR band shapes are similar to those for the regular models, with less amide I splitting than the planar but more than the supercoiled antiparallel β-sheet. Similarly to the supercoiled models, the amide I IR intensity in the twisted β-sheets is also more distributed over several lower frequency transitions, rather than being concentrated predominantly in the lowest frequency mode as in the planar antiparallel case. Both of these twisted β-sheet segments are predicted to have a much stronger amide I VCD than the planar sheet, with a lower frequency positive couplet band shape, and a weaker negative couplet to high frequency. Most transitions contribute intense rotational strengths (as indicated by vertical positive and negative lines) that tend to be dispersed in an alternating pattern of positive and negative signs, which leads to cancellation of the overall VCD. Despite this, the amide I VCD retains substantial intensity but is weaker than the amide I VCD of the supercoiled β-sheet (Figure 6), where the cancellation is smaller. The amide II VCD retains band shapes roughly similar to those of the regular models, as do the amide III IR and VCD.

Twisted Parallel β-Sheets. The simulated spectra of pentaamide segments of the pectate lyase, in two-, three-, and five-stranded parallel β-sheet configurations, are shown in Figure 8. The IR amide I band shapes closely resemble those in the planar parallel β-sheets with the main maxima at slightly higher frequency. We note, however, that higher amide I frequency and correspondingly less amide I component splitting may be partly due to the shorter length (pentaamide) of the twisted β-sheet model as compared to the planar (octaamide) one. In the three- and five-stranded models, the central component of the amide I is more significant than in the planar models, tending to broaden the spectra. A much lower effect of the twist is predicted for the parallel β-sheet VCD as compared to the large enhancement of the VCD intensity upon sheet twist for the antiparallel sheets. However, in both twisted and planar parallel cases, the sense of the VCD corresponding to the lowest frequency IR amide I component is opposite (negative) that of the twisted antiparallel models (positive to lowest frequency, Figure 7).

Discussion

Our previous computational studies of model helical structures evidence good qualitative agreement with experiment for α-helical, 3_{10}-helical (relative), and 3_1 (ProII-like)-helical IR and VCD.[6,29,31,41] Errors in the predicted rotational strengths due to small variations of the structure and inadequacies of the computational method are expected to be small compared to the overall predicted VCD intensity, and therefore have little effect on the helical VCD band shapes. On the other hand, for β-sheets, while the IR spectral simulations are likely to be reasonably accurate, due to the inherently weak VCD, structure and method errors of the same magnitude may have significant consequences on the computed band shape. This is made clear here in the high sensitivity of the simulated VCD to twist for the antiparallel structures. Thus, in the β-sheet case, rather than

(40) Dukor, R. K.; Keiderling, T. A. *Biopolymers* **1991**, *31*, 1747.

(41) Silva, R. A. G. D.; Yasui, S. C.; Kubelka, J.; Formaggio, F.; Crisma, M.; Toniolo, C.; Keiderling, T. A., submitted for publication.

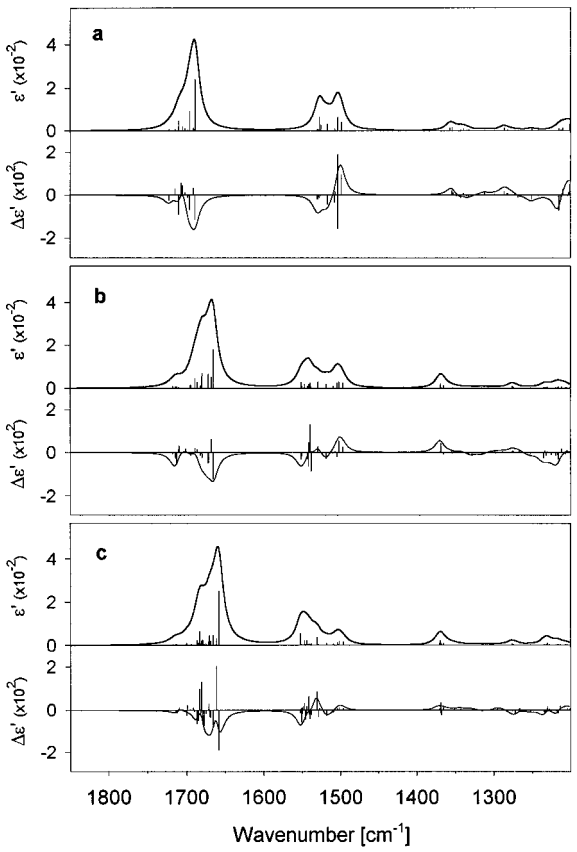

Figure 8. Simulated IR and VCD spectra by transfer of parameters for parallel β-sheet structure based on a segment of β-helix protein pectate lyase (2PEC, Table 1), by transfer of parameters from ab initio calculations. (a) Two-stranded β-sheet, (b) three-stranded β-sheet, (c) five-stranded β-sheet, all with pentaamide strands (Ac-A_4-NH-CH_3). Spectral intensity units (ϵ', $\Delta\epsilon$') as in Figure 3.

the detailed band shape pattern, the predicted magnitude and the overall sign of the VCD signal is likely to be the experimental variable that can be reliably structurally interpreted. As the above results demonstrate, the VCD magnitude does depend on the detailed conformation of the β-sheet, such as parallel or antiparallel arrangement of the strands and the sheet twist.

Number of Associated, Hydrogen-Bonded β-Strands. For all model structures, on forming a multiple-stranded sheet the amide I shifts to the lower frequency compared to a single strand, while the amide II shifts up, reducing the amide I−II separation to one better approaching the experimental value (∼100 cm^{-1}). These frequency shifts correlate with added hydrogen bonding, since the hydrogen bond reduces the force constant of the C═O stretching (amide I) vibration and increases that of the N−H (amide II) bending motion. Hydrogen bonding causes the amide II to become split into two main components corresponding to hydrogen bond donor amides (higher frequency) and those that are not (lower frequency). Unlike the amide II, the low- and high-frequency amide I modes cannot be simply related to the hydrogen bonding of the amide C═O groups, even though the lowest frequency modes generally arise from innerstrand amide groups. The frequency distribution in the amide I mode depends more on the phase of the particular mode, which accounts for the splitting and intensity distribution in the single-stranded peptides.

The second significant effect of added strands is on the relative amide I and II IR intensities. While the amide II of a single strand is generally stronger than its amide I, in the multiple-stranded sheets the opposite is true. The amide I intensity undergoes significant enhancement by coupling the vibrations on different β-strands. Amide II modes, on the other hand, are relatively localized on a single strand with some loss in the absolute intensity. With increasing the number of strands, both the amide I and amide II bands broaden, offering further evidence of a strong coupling between local modes that is enhanced by interstrand coupling. While it is tempting to ascribe this to H-bonding, our results suggest that it is more complex. Because the split character of the IR amide I band is observed in the single-stranded simulations, it cannot be solely due to the hydrogen bonding. This would be consistent with findings of Moore and Krimm,[42] who empirically added nonbonded, transition dipole coupling (TDC) interactions to the force field in order to explain this band shape. However, as also pointed out,[43,44] perturbative treatments based on TDC alone[25,42,45] are not sufficient to explain certain important details of amide I spectra.

We performed a series of test calculations on the small three-stranded β-sheet using a transferred ab initio FF from *N*-methylacetamide for each amide group and the TDC correction based on the ab initio values of transition dipole strengths (APT)[29,32] as coupling terms. Such a test does not require any empirical parameters. Alternatively, the ab initio FF from a single-strand calculation was transferred and the TDC used only for interstrand coupling. Spectra thus obtained were compared to those from the full ab initio calculation (Figure 3d). These tests show that if the splitting were due only to the TDC, the high-frequency amide I components would shift farther up and the lower frequency ones farther down, thus maintaining the center frequency of the band. On the other hand, in the ab initio simulations both components shift to the lower frequencies (the high frequency one only slightly) as more strands are added. Furthermore, the component splitting is significantly underestimated if only the TDC is included, as based on the ab initio APT values (transition dipoles), even though the calculated APT magnitudes are approximately correct, since they yield approximately correct IR intensities. Therefore, both bonded and nonbonded interactions are necessary for prediction of proper IR band shapes. This ab initio-based result is consistent with recent empirical parametrized calculations by Mendelsohn and co-workers that required both through-bond (including H-bonds) and TDC interactions to reproduce the amide I band shapes of ^{13}C isotopically labeled β-sheet oligopeptides.[46]

Depending on the conformation, the predicted VCD band shapes show different behaviors when the number of strands of the model peptide increases. Amide I VCD generally conserves its overall shape and intensity, being much more dependent on the strand conformation than the number of associated strands. However, a general trend appears in the amide II VCD band shape. Single strands have negative couplet amide II VCD (with widely varying intensity), which changes into a complex band shape for the multiple-stranded sheets, where the components often have a positive couplet shape dispersed over the components.

Conformations of the β-Sheet. The most pronounced splitting of the amide I along with its lowest frequency

(42) Moore, W. H.; Krimm, S. *Proc. Natl. Acad. Sci. U.S.A.* **1975**, *72*, 4933.
(43) Lee, S. H.; Krimm, S. *Chem. Phys.* **1998**, *230*, 277.
(44) Krimm, S. In *Infrared Analysis of Peptides and Proteins: Principles and Applications*; Singh, B. R., Ed.; ACS Symposium Series; American Chemical Society: Washington, DC, 2000; p 38.
(45) Torii, H.; Tasumi, M. *J. Chem. Phys.* **1992**, *96*, 3379.
(46) Brauner, J. W.; Dugan, C.; Mendelsohn, R. *J. Am. Chem. Soc.* **2000**, *122*, 677.

maximum is predicted for the planar, multistranded antiparallel models, which correspond to aggregated β-sheets in polypeptides, denatured proteins, and certain model oligopeptides.[32] Parallel (being more pleated) and twisted β-sheets are predicted to have significantly smaller amide I splitting along with a higher frequency for the lower component maxima. In twisted antiparallel β-sheets, this higher frequency of the amide I absorption maximum is due not only to less frequency splitting of the amide I modes, but also to the fact that the lowest frequency amide I mode is not the most intense, in contrast to the planar antiparallel β-sheet. Both pleat and twist of the sheet thus decrease the effect of interstrand coupling (since under their influence the splitting does not as greatly change with strand number) of the amide I modes, which is responsible for the characteristic, split amide I absorption band shape seen in more extended sheets. By contrast, the amide II, which is more localized on one strand, shows similar splitting (assuming the same number of strands) in all structures.

More significant differences between the conformational models are observed in the simulated VCD. The VCD of all β-sheet models is weak compared to that of the helical structures. The fully extended (all-trans) conformation would have a plane of symmetry with respect to the amide groups (neglecting the chiral C^{α} configuration), since all amide groups are in the same plane. The chirality of the amide chain (viewed in isolation from the C^{α} links) is therefore lost, and, in principle, the VCD should vanish. In such a structure, considering only amide modes, the electric and magnetic transition dipole moments would be orthogonal, and thus the rotational strength, $R = \mathrm{Im}\langle \boldsymbol{\mu}\cdot\mathbf{m}\rangle$, would be zero. A pleated sheet no longer has the planar symmetry, and there can be a nonzero magnetic moment component that projects on the electric transition dipole moment, even though the strand is a 2_1-helix (two residues per turn). The VCD is therefore expected to increase with the pleat of the sheet and does so in our calculations. The twist adds more local helical character to the structure and therefore would be expected to cause significant enhancement of the VCD signals, particularly for the less pleated, antiparallel sheet, again as we calculate.

The planar antiparallel β-sheet structures exhibit the weakest amide I VCD with inherently small rotational strengths in all transitions. The predicted VCD intensity (per amide group) actually decreases somewhat with the size of the β-sheet both in length and, particularly, in number of strands. Amide II intensity decreases drastically when the number of strands is increased. The structure becomes effectively less chiral as it becomes larger, since the proportion of dipole components perpendicular to the sheet plane decreases. The planar parallel β-sheet predicts more amide I VCD intensity, virtually all negative, that stays roughly constant (per residue) with increasing number of strands. The increased intensity, as compared to antiparallel, derives from the increased pleat in the parallel strand. This dominantly negative VCD is not obviously balanced by positive VCD elsewhere, which must represent an intrinsic local chirality resulting from the increase in pleating.

Twisted antiparallel structures exhibit much more intense amide I VCD signals. The supercoiled β-sheet amide I VCD is the strongest found for all the simulated models and resembles that computed (and observed) for a left-handed 3_1-helix.[6,29,31,40,47] This β-coil amide I VCD band shape is a consequence of the twisting of each strand in a left-handed sense, deforming the 2_1 (extended) conformation in the direction of the left-handed 3_1-helix.

The twisted, protein-based, antiparallel β-sheet models show more intense amide I VCD signals than do the planar antiparallel β-sheets, but less intensity than for the supercoiled structures. The amide I VCD band shapes are quite surprisingly different from those of the supercoiled sheets, even though the strands in both conformations correspond to locally left-handed helices.[1,2] Presumably this is evidence of the impact of sensitivity to small structural variations for a small calculated VCD. The parallel twisted β-sheet amide I VCD is of similar intensity and the same sign pattern as the planar model. Due to the larger VCD intensity stemming from its more pleated, less extended conformation, predicted VCDs for the parallel β-sheets are less affected by twist. Both show the lowest frequency component of the amide I, which is most intense in the IR, to have an overall negative VCD, while for the twisted antiparallel case the lowest component is positive. Whether this could discriminate between the parallel and antiparallel β-sheets is an open question given some doubt by the β-coil results. Contrary to the antiparallel cases, the parallel twist actually slightly decreases rather than increases the amide I VCD, owing to more cancellation of oppositely signed transitions in the twisted structures. Here the key to the difference is that perturbations (such as degree of twist) show their largest effects when the unperturbed spectrum is very weak, as in the planar antiparallel case.

Comparison with Experimental Data. Comparison of the simulated spectra with experimental data is difficult due to the previously discussed scarcity of simple β-sheet models. While some polypeptides, such as poly(K) and poly(LK), under certain conditions form aggregated β-sheets[26−28,48] whose spectra can be compared to the planar, large antiparallel simulations, similar suitable peptide models for twisted and parallel β-structures are not available, and the comparison can be only made to the protein spectra.

Experimental IR and VCD spectra for the poly(LK) peptide under high salt conditions (amide I in D_2O and amide II in H_2O) and for highly β-sheet-containing proteins, concanavalin A and superoxide dismutase (in H_2O only), are shown in Figure 9. Poly(LK) under high salt conditions forms a β-sheet structure, most likely an aggregate of antiparallel strands, such as is well-known for many polypeptides.[26,28,32,46,49−53] Concanavalin A (conA) contains about 40% β-structure[54] in large, relatively flat (for a protein) multiply stranded antiparallel sheets. Superoxide dismutase (sod) contains about 30% of β-sheet structure[55] assembled in smaller, twisted antiparallel sheets that more closely resemble the β-barrel domain of the fatty acid binding protein.[34]

Both the IR and VCD amide I spectra of poly(LK) (Figure 9a) are in best agreement with the simulations for the largest, five-stranded antiparallel planar β-sheet model (Figure 4d). The key points of comparison are the large splitting of the weak high-frequency amide I component and the intense low-frequency one, and the relative intensity of these components. The moderate intensity band between them in the simulation is

(47) Dukor, R. K.; Keiderling, T. A.; Gut, V. *Int. J. Pept. Protein Res.* **1991**, *38*, 198.
(48) Greenfield, N.; Fasman, G. D. *Biochemistry* **1969**, *8*, 4108.
(49) Jackson, M.; Haris, P. I.; Chapman, D. *Biochim. Biophys. Acta* **1989**, *998*, 75.
(50) Caughey, B. W.; Dong, A.; Bhat, K. S.; Ernst, D.; Hayes, S. F.; Caughey, W. S. *Biochemistry* **1991**, *30*, 7672−7680.
(51) Haris, P. I.; Chapman, D. *Biopolymers* **1995**, *37*, 251.
(52) Dong, A. C.; Prestrelski, S. J.; Allison, S. D.; Carpenter, J. F. *J. Pharm. Sci.* **1995**, *84*, 415−424.
(53) Khurana, I.; Fink, A. L. *Biophys. J.* **2000**, *78*, 994.
(54) Naismith, J. H.; Habash, J.; Harrop, S.; Helliwell, J. R.; Hunter, W. N.; Wan, T. C. M.; Weisgerber, S.; Kalb, A. J.; Yariv, J. *Acta Crystallog. D, Biol. Crystallog.* **1993**, *49*, 561.
(55) Tainer, J. A.; Getzoff, E. D.; Beem, K. M.; Richardson, J. S.; Richardson, D. C. *J. Mol. Biol.* **1982**, *160*, 181.

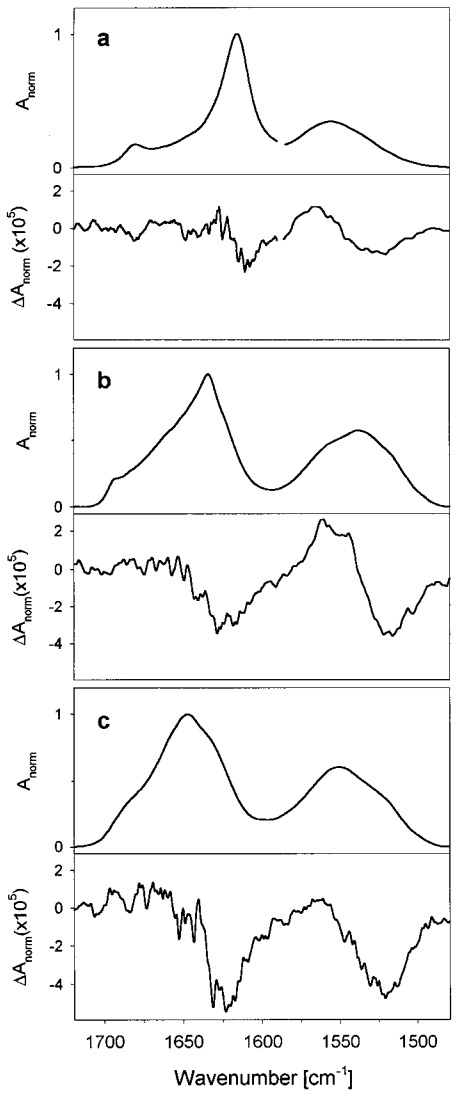

Figure 9. Experimental β-sheet IR and VCD spectra in amide I and amide II region. (a) Poly(LK) (amide I in D_2O, amide II in H_2O), (b) concanavalin A in H_2O, and (c) superoxide dismutase in H_2O.

a result of non-hydrogen-bonded C═O groups on the edge strands (see below) which are not actually relevant to the solution phase or to any highly aggregated molecules.

The amide I IR of conA (Figure 9b) has features somewhat between those simulated for the three-stranded planar (Figure 4c) and three-stranded twisted antiparallel β-sheet (Figure 7b). Here the defining characteristics are a relatively sharp major feature at ~1635 cm^{-1} and a much weaker one at ~1690 cm^{-1}, significantly less split than for poly (LK). There is much more intensity between these features than predicted in the simulations, but the β-sheet nature is very clear in conA. By contrast, the amide I IR of sod (Figure 9c) is quite broad, with its most intense feature at ~1648 cm^{-1}, lying between two shoulders corresponding to more typical β-sheet frequencies at ~1635 and ~1685 cm^{-1}. It is important to recognize that these protein structures have <50% β-sheet content, and other local structures contribute to the IR, several of which will have transitions between the high- and low-frequency β-sheet features. The difference in the IR between the two proteins is consistent with conA having larger and more planar β-sheets which yield a larger separation between the dominant amide I components. Amide I VCD spectra for both these β-sheet proteins (Figure 9b,c) show a negative minimum on the low-energy side of the IR band. Simulated amide I VCD predicts this overall negative amide I VCD but not its detailed mode pattern. The amide I VCD is more intense in sod than in conA, which again would be consistent with the different size and relative degree of twist of the β-sheet in these two proteins.

It is important to note that the amide I VCD negative maximum is in all cases shifted toward lower frequency from the IR absorption maximum. In the antiparallel planar β-sheet simulations, the IR maximum essentially corresponds to the lowest frequency amide I transition; thus, there cannot be any transition at lower frequency corresponding to the VCD negative maximum. By contrast, in the twisted sheets the absorption maximum no longer corresponds to the lowest frequency amide I transition, and thus such a pattern is possible. Alternately, if the lower frequency transitions give rise to a couplet shape, the lowest frequency lobe will tend to appear on the low-frequency side of the absorbance maximum. That this lowest frequency negative VCD is not seen in our antiparallel, twisted β-sheet simulations can be due to inaccuracies in calculated rotational strengths but may also arise due to residues in other (e.g., turn, loop) conformations, which can have considerable VCD intensity. Overlap of these contributions can lead to considerable broadening of the amide I and definite uncertainty as to what band shape aspects to separate out and attribute to the β-sheet structure. In fact, our preliminary results from spectral simulations for β-turns and β-hairpins suggest that the lowest frequency amide I transitions in these models originate from Pro-containing turn segments.[56] It is interesting to note that the two proteins in Figure 9 contain Pro residues in their loop and turn regions.

Experimental amide II IR does not show the split band predicted by the simulations, but its shape suggests multiple components. We note that in 2-D correlation analyses of a training set of protein spectra (including these proteins) with respect to their secondary structure contents,[57,58] two distinct components for the amide II were identified that correlated with β-sheet content. The amide II VCD has in all cases a broad negative couplet sign pattern which, while in agreement with the single-stranded simulations, does not reflect the multi-stranded simulations. This discrepancy may be partly due to the distorted strand ends for real β-sheet structures formed from a single polypeptide chain but is mostly due to the lack of solvent in our simulations. Normal-mode analysis shows that the highest frequency antiparallel amide II modes, those with negative VCD, are localized on the hydrogen-bonded N-terminal amide groups of the β-strands. In the real polypeptide sample, since these residues couple to turns or loops, they must be distorted. The low-frequency amide II components, on the other hand, arise from the amides on the outer strands of the β-sheet whose N−H groups point outward and do not hydrogen bond in our isolated peptide model. Experimentally, the amide II spectra are very broad, showing little structure which is consistent with there being a significant solvent effect on the shape.

To test the effect of differential H-bonds on the outside strands in our model above, we recalculated the three- and five-strand planar antiparallel sheet by transferring parameters only from the center strand (all H-bonded) of the three-stranded small-molecule model. In these simulations, the amide II IR indeed became a broadened single band. In addition, the amide I IR

(56) Hilario, J.; Kubelka, J.; Syud, F. A.; Gellman, S. H.; Keiderling, T. A. *Biospectroscopy* **2001**, in press.

(57) Pancoska, P.; Kubelka, J.; Keiderling, T. A. *Appl. Spectrosc.* **1998**, *53*, 655.

(58) Kubelka, J.; Pancoska, P.; Keiderling, T. A. *Appl. Spectrosc.* **1998**, *53*, 666.

shifted slightly down in frequency, and the center feature became much weaker (barely noticeable in the band shape profile). Both VCD simulations had all negative amide I (largest intensity to lower wavenumber), and the amide II became a single positive couplet. The latter does not agree with the experimental data, however. Our results thus suggest that amide II IR and VCD would be much less useful than the amide I for discriminating between structures. In fact, this is what we have found experimentally.[59,60]

The comparison for parallel β-sheets is practically impossible, since no polypeptide models are known. In proteins, most parallel β-sheets are found in α/β motifs, whose comparatively large α-helical content would position an intense IR band in the center of any split β-sheet components and would dominate the VCD spectra. The recently identified β-helix and β-roll structures,[1] which contain little or no α-helix, are the exception. VCD spectra for β-helix or β-roll proteins are currently not available. However, the amide I IR spectra for three β-helix proteins, the P22 tailspike protein,[61] UDP-*N*-acetylglucosamine acyltransferase,[62] and pectate lyase C,[35] have been reported.[53] All three proteins, prepared as hydrated thin films (H_2O) and measured with ATR techniques, have a broad amide I contour with a maximum at $\sim$1640 cm^{-1} and weaker, partially resolved components as high as $\sim$1690 cm^{-1}. These band shapes agree with the calculated amide I IR band shape for the twisted parallel β-sheet, whose structure was in fact based on a segment of one β-helix protein, pectate lyase C. By contrast, the reported IR spectra for the KLKLKLELELELG peptide (KLEG),[63] which was thought to form β-helical fibrils due to its alternating hydrophobic−hydrophilic nature,[64] are totally consistent with extended, multistranded antiparallel sheets (main maximum $\sim$1623 cm^{-1}).[53] The IR amide I of KLEG is almost identical to the previously reported $K_2(LA)_6$ results[32,46] and quite similar to that of poly(LK)[28] (Figure 9a) and to the multistranded, antiparallel planar simulations (Figure 4d). Our results thus support the conclusion of Khurana and Fink[53] that KLEG is not a β-helix and show that it forms an extended antiparallel β-structure, the only β-structure with a unique amide I IR intensity pattern.

In summary, it seems that the simulated IR for appropriate models is in much better agreement with experiment than is the VCD. This underlines the sensitivity of VCD to the conformational details, such as unknown detailed conformations of the terminal strands and strand ends of the multistranded β-sheet aggregates in solution. While we have not found a general discrimination between parallel and antiparallel β-sheets, we have found a specific one. The often seen IR spectral pattern of a very intense amide I band at $\sim$1620 cm^{-1} and a weak band at $\sim$1690 cm^{-1} fits only the simulation for extended, multistranded antiparallel β-sheets. All parallel and twisted forms have much less amide I splitting. Since this describes the general situation in globular proteins, our results suggest significant difficulties in discriminating β-sheet types in proteins. The nonuniformity of sheets as compared to helices leads to a nonuniform spectral response for the class of β-sheet structures, but once the details are better understood, there is a hope for further discrimination between various structures using IR and VCD techniques.

Acknowledgment. This work was supported in part by grants from the donors of the Petroleum Research Fund, administered by the American Chemical Society, and by the Research Corporation for which we are most grateful. J.K. was supported as a UIC Dean's Scholar. We thank Prof. Richard Mendelsohn for initial discussion of β-sheet peptides, Prof. Stefan Franzen for discussing comparative computational results, both before publication, and Dr. Sergei Venyaminov for pointing out some earlier computational results.

JA0116627

(59) Gupta, V. P.; Keiderling, T. A. *Biopolymers* **1992**, *32*, 239.
(60) Pancoska, P.; Bitto, E.; Janota, V.; Keiderling, T. A. *Faraday Discuss.* **1994**, *99*, 287.
(61) Steinbacher, S.; Seckler, R.; Miller, S.; Steipe, B.; Huber, R.; Reinemer, P. *Science* **1994**, *265*, 383.
(62) Raetz, C. R.; Roderick, S. L. *Science* **1995**, *270*, 997.
(63) Lazo, N. D.; Downing, D. T. *Biochem. Biophys. Res. Commun.* **1997**, *235*, 675.
(64) Downing, D. T. *Proteins* **1995**, *23*, 204.